ISSN 0967-859X
THE SOCIETY FOR EARTHQUAKE AND CIVIL ENGINEERING DYNAMICS

NEWSLETTER

Volume 21 No 1
November 2008

In this issue

A new boundary condition for analysis of semi-infinite media in time domain

Andreas H Nielsen
Jacobs, Glasgow

Email: andreas.nielsen@jacobs.com

Introduction

Civil engineers use computer simulations to predict the response of structures to earthquake excitation. The seismic waves generated by a typical earthquake can propagate several times around the earth. However, computer models are usually truncated at a relatively small distance from the region of interest. The presence of ground outside the artificial borders of the model is then approximated numerically by a boundary condition.

The effect of any boundary condition on the local response may be expected to diminish with distance according to Saint-Venant's principle. In static problems, fixed or free boundary conditions can be used at a relatively small distance from the region of interest without sacrificing much in terms of accuracy. However, in dynamic problems, these elementary boundary conditions cause the reflection of outward propagating (radiating) waves, effectively trapping seismic energy inside the model. The simplest solution to this problem is to define a large enough model so that waves reflected at the artificial boundaries do not have time to return to the region of interest (e.g. a structure on the surface) although, due to the relatively high wave speeds of most geological media, this is rarely a practical option. It is desirable therefore to have boundary conditions that allow the necessary radiation of energy.

Boundaries that do not reflect waves are called by various names: radiation boundaries, quiet boundaries, transmitting boundaries, absorbing boundaries, etc. Numerous solutions have been proposed in the past 35 years, and the literature on the subject is vast. Cohen and Jennings (1983), Wolf (1988) and Mulder (1997) all provide good introductions. A selective review of various solutions is provided here.

Most absorbing boundary conditions (ABCs) can be classified in two broad categories: global and local. In a global scheme, each boundary node (or gridpoint) is fully coupled to all other boundary nodes in both space and time. In a local scheme, the solution at any time step depends only on the current node and the current time step, and perhaps a few neighbouring points in time and space. Generally speaking, global boundaries are exact, but limited in their applications; local boundaries are approximate, but are much more attractive for numerical implementation than global boundaries.

The first local ABC was the viscous boundary due to Lysmer and Kuhlemeyer (1969). The boundary condition is completely effective at absorbing body waves approaching the boundary at normal incidence. For oblique angles of incidence, or for surface waves, there is still energy absorption, but it is not perfect. The viscous boundary is easy to implement in most general purpose finite element codes and, for that reason, it remains one of the most popular methods today.

Solutions published after 1969 are based on a variety of techniques. Several authors have aimed to devise a convenient mathematical approximation to the one-way wave equation, i.e. a governing equation that allows wave propagation in one direction only. One of the first solutions of this kind, and still one of the most accurate, was proposed by Lindman (1975) for the acoustic wave equation and extended by Randall (1988) to the elastic wave equation. The Lindman boundary absorbs both body and surface waves with equal efficiency. However, the procedure is developed for finite difference calculations and is not easily transferred into a finite element setting.

The paraxial boundary, which appeared in 1980's, was an attempt to implement the one-way wave equation in a finite element setting. In this method (Cohen and Jennings, 1983; Wolf, 1988), the governing one-way wave equation is recast in weak form; the weak form is integrated, and the structural matrices of a paraxial finite element are obtained. A boundary layer of paraxial elements around the main model works as an ABC. In theory, the paraxial boundary should more accurate than the viscous boundary, but actual results show that, in practice, the improvement is slight (Cohen and Jennings, 1983).

Kellezi (2000), in effect using the same cone models as proposed by Wolf (1994), derived a local, doubly-asymptotic ABC. In this method the dashpots used to implement the standard viscous boundary are supplemented by springs. The stiffness of each spring is a function of radial distance r from an internal source of excitation; what value r should be given when the seismic source is external to the model is not clear although some guidance is given by Kontoe, Zdravkovic and Potts (2008). Numerical evidence seems to suggest that the 'cone boundary' performs better than the viscous boundary, but the actual difference between the two methods is not large.

In a recent paper Guddati (2006) derived a series of approximations to the one-way wave equation with increasing accuracy. The procedure is applicable to various types of material including anisotropic and porous elastic media, and it provides effective energy absorption over an arbitrarily wide range of incident angles. The basic idea is to expand the governing one-way equation by means of a continued fraction; this approximation contains a number of auxiliary variables, which are interpreted as additional degrees of freedom and enter the global system of equations alongside the conventional degrees of freedom. As such, the application of the boundary condition can be viewed as adding layers of elements around the artificial boundaries of the model where energy radiation is required. One layer of elements provide perfect absorption of incident waves with wavenumber k when the 'length' L of the absorping layer is defined as $L = 2i/k$ where $i = \sqrt{-1}$. When L is imaginary (k real), the layer captures mainly body waves. When L is complex, the layer absorps both body and surface waves. By adding more layers with different L values, the method becomes increasingly accurate for all types of waves. The use of complex numbers to define the properties of an element results in complex system matrices. Therefore, the implementation of this boundary condition in a time domain algorithm requires some effort. Also, the choice of optimal 'lengths' (L) will vary from one problem to another and could require additional effort. For that reason, more work is needed to increase the practical appeal of this boundary condition.

This article proposes a new ABC for analysis in time domain. The solution promises to provide an exact, and yet relatively simple ABC for time domain analysis. The theory behind the ABC is derived in the following sections. Possible methods of implementation are discussed; and a number of potential advantages and problems are identified.

At this point in time, due to other commitments, the author has not obtained any numerical results to validate the ABC. Therefore, a request for further work is put forward. More to the point, it is believed that implementation and validation of the ABC could be suitable material for a (demanding) final year MSc project or form part of a related PhD project.

Naturally, the author would also like to hear from anyone who can perceive flaws in the proposed method, or suggest improvements.

Basic theory of wave propagation in elastic media

The wave equation for an isotropic elastic medium may be written as (Love, 1944)

$$c_p^2 \nabla(\nabla \cdot \boldsymbol{u}) - c_s^2 \nabla \times \nabla \times \boldsymbol{u} = \frac{\partial^2 \boldsymbol{u}}{\partial t^2} \tag{1}$$

where c_p and c_s are constants defined below, and $\boldsymbol{u}$ is the displacement vector,

$$\boldsymbol{u} = (u, v, w).$$

In an infinite medium, the wave equation (1) admits two and only two types of wave motion: primary (P) waves and secondary (S) waves. These waves propagate independently of each other and at different speeds. The P-wave speed is given by

$$c_p = \sqrt{\frac{\lambda + 2\mu}{\rho}}, \tag{2}$$

and the S-wave speed is given by

$$c_s = \sqrt{\frac{\mu}{\rho}}, \tag{3}$$

where μ and λ are the Lamé constants, and ρ is the density. Both P- and S-waves are classified as body waves. The P-wave is a dilatational wave involving no rotation ϖ, and the S-wave is a shear wave involving no dilatation Δ. In mathematical notation,

$$\text{for P-waves:} \quad \varpi = 0, \tag{4a}$$
$$\text{for S-waves:} \quad \Delta = 0, \tag{4b}$$

where, for 2D plane strain wave propagation,

$$\Delta = \frac{\partial u}{\partial x} + \frac{\partial v}{\partial y}, \tag{5a}$$
$$\varpi = \frac{1}{2}\left(\frac{\partial v}{\partial x} - \frac{\partial u}{\partial y}\right). \tag{5b}$$

Note that both of these quantities are invariants and, hence, do not depend on the orientation of the chosen coordinate system.

Where a natural boundary exists, the wave equation admits another class of waves called evanescent waves. These waves travel along the boundary between two media — in particular a free surface, in which case the term surface waves also applies. The motion decays exponentially in the direction normal to the boundary. Combinations of possible boundary conditions lead to a variety of these waves. In general, evanescent waves are dispersive, i.e. the wave velocity depends on frequency.

Boundaries not only act as waveguides for evanescent waves, they also couple the otherwise independently propagating dilatational and shear wave. It follows that the real difficulty in simulating seismic wave propagation not so much lies in the interior of the model, but at the artificial boundaries. In the following it is assumed that evanescent waves are absent from the problem at hand.

Two types of conditions must be satisfied on the surface of a wave front: kinematical and dynamical conditions (Love, 1944). Restricting ourselves to the two-dimensional case, kinematical conditions may be written as

$$\frac{1}{\cos\theta}\frac{\partial u}{\partial x} = \frac{1}{\sin\theta}\frac{\partial u}{\partial y} = -\frac{1}{c}\frac{\partial u}{\partial t}, \tag{6a}$$
$$\frac{1}{\cos\theta}\frac{\partial v}{\partial x} = \frac{1}{\sin\theta}\frac{\partial v}{\partial y} = -\frac{1}{c}\frac{\partial v}{\partial t}, \tag{6b}$$

where θ is the angle of incidence (see Figure 1), and c is the wave speed.

Dynamical conditions are given by

$$\rho c\frac{\partial u}{\partial t} = -f_x, \tag{7a}$$
$$\rho c\frac{\partial v}{\partial t} = -f_y, \tag{7b}$$

where f_x and f_y are tractions applied to the surface dS of the interface, which is assumed to be coplanar with the wave front (see Figure 1).

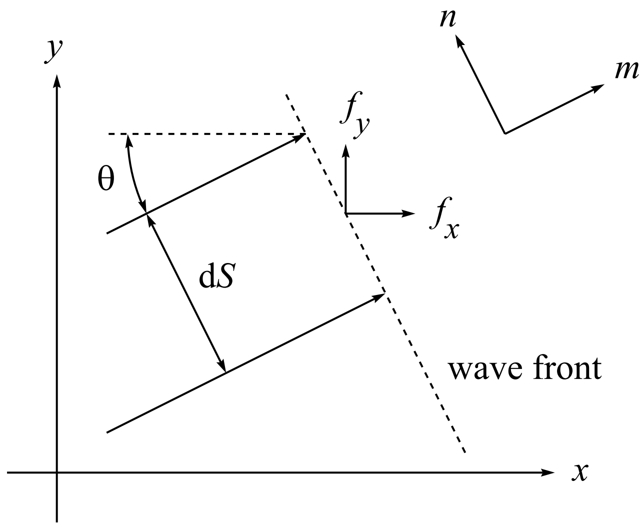

Figure 1: Definition sketch

A new ABC for analysis in time domain

Derivation

Consider first a plane P-wave approaching the boundary $x = a$ with incident angle θ_p. In the coordinate system defined by (m, n) in Figure 1, the direct stress evaluated at the boundary is given by

$$\sigma_m = f_x \cos\theta_p + f_y \sin\theta_p. \tag{8}$$

As a P-wave propagates through an elastic medium, it causes only displacement in the direction of propagation. The plane perpendicular to the wave vector remains in a state of zero strain as the P-wave travels through the medium ($\epsilon_n = \epsilon_z = 0$). It follows from Hooke's law that

$$\sigma_n = \frac{\nu}{1-\nu}\sigma_m = \frac{\lambda}{\lambda+2\mu}\sigma_m. \tag{9}$$

There is no shear stress in the coordinate system (m, n), as the directions of principal stress coincide with (m, n). The stress in the main coordinate system (x, y) is given by

$$\sigma_x = \frac{1}{2}(\sigma_m + \sigma_n) + \frac{1}{2}(\sigma_m - \sigma_n)\cos 2\theta_p, \tag{10a}$$

$$\tau_{xy} = \frac{1}{2}(\sigma_m - \sigma_n)\sin 2\theta_p. \tag{10b}$$

In order to simplify notation, define

$$\eta = \frac{\lambda}{\lambda+2\mu}.$$

Substituting (8) and (9) into (10) gives

$$\begin{aligned}\sigma_x &= \frac{1}{2}(f_x\cos\theta_p + f_y\sin\theta_p)\left[(1+\eta)\right.\\ &\quad \left.+ (1-\eta)\cos 2\theta_p\right],\\ \tau_{xy} &= \frac{1}{2}(f_x\cos\theta_p + f_y\sin\theta_p)(1-\eta)\sin 2\theta_p.\end{aligned}$$

Then, using dynamical conditions (7), the stress can also be written as

$$\begin{aligned}\sigma_x &= -\frac{\rho c_p}{2}\left(\frac{\partial u}{\partial t}\cos\theta_p + \frac{\partial v}{\partial t}\sin\theta_p\right)\left[(1+\eta)\right.\\ &\quad \left.+ (1-\eta)\cos 2\theta_p\right],\\ \tau_{xy} &= -\frac{\rho c_p}{2}\left(\frac{\partial u}{\partial t}\cos\theta_p + \frac{\partial u}{\partial t}\sin\theta_p\right)(1-\eta)\sin 2\theta_p.\end{aligned}$$

Substituting kinematical conditions (6) into the above equations yields

$$\begin{aligned}\sigma_x &= \frac{\rho c_p^2}{2}\left(\frac{\partial u}{\partial x} + \frac{\partial v}{\partial y}\right)\left[(1+\eta) + (1-\eta)\cos 2\theta_p\right],\\ \tau_{xy} &= \frac{\rho c_p^2}{2}\left(\frac{\partial u}{\partial x} + \frac{\partial v}{\partial y}\right)(1-\eta)\sin 2\theta_p,\end{aligned}$$

or, using (2) and (5a),

$$\begin{aligned}\sigma_x &= \frac{1}{2}(\lambda+2\mu)\Delta\left[(1+\eta) + (1-\eta)\cos 2\theta_p\right],\\ \tau_{xy} &= \frac{1}{2}(\lambda+2\mu)\Delta(1-\eta)\sin 2\theta_p.\end{aligned}$$

Hence, it may be verified that σ_x and τ_{xy} can also be written as

$$\sigma_x = \Delta\left(\lambda + \mu(1+\cos 2\theta_p)\right), \tag{11a}$$

$$\tau_{xy} = \Delta\mu\sin 2\theta_p. \tag{11b}$$

Consider next a plane S-wave approaching the boundary $x = a$ with incident angle θ_s. In this case, there is no direct stress in the coordinate system (m, n). The shear stress is given by

$$\tau_{mn} = f_y\cos\theta_s - f_x\sin\theta_s,$$

which leads to

$$\sigma_x = -(f_y\cos\theta_s - f_x\sin\theta_s)\sin 2\theta_s, \tag{12a}$$

$$\tau_{xy} = (f_y\cos\theta_s - f_x\sin\theta_s)\cos 2\theta_s. \tag{12b}$$

Using the same procedure as above to manipulate the right hand side of (12), we arrive at the following expressions for the boundary tractions due to incident S-wave:

$$\sigma_x = 2\varpi\mu\sin 2\theta_s, \tag{13a}$$

$$\tau_{xy} = -2\varpi\mu\cos 2\theta_s. \tag{13b}$$

It may be verified analytically that if (11) and (13) are added and applied as boundary tractions, the reflection coefficients are zero for all incident angles (a Maple worksheet that demonstrates this is available on request from the author). It should be noted that (11) evaluates to zero for incident S-wave; likewise, (13) is zero for incident P-wave (cf. (4) and (5)).

Estimation of incident angle

Crucial to the implementation is the numerical evaluation of the incident angle θ. This section proposes a method for determining this angle. Other methods may be considered.

The dilatation and the rotation satisfy two independent scalar wave equations (Love, 1944), each of which may be written as

$$\frac{\partial^2\phi}{\partial t^2} = c^2\nabla^2\phi \tag{14}$$

where it is implied that

$$\begin{aligned} c &= c_p \quad \text{for} \quad \phi = \Delta,\\ c &= c_s \quad \text{for} \quad \phi = \varpi.\end{aligned}$$

The scalar wave equation (14) can be reduced to a one-way wave equation

$$\frac{\partial\phi}{\partial t} + \frac{c}{\cos\theta}\frac{\partial\phi}{\partial x} = 0, \tag{15}$$

which for angles in the range $\theta \in [-90; 90]$ allows propagation in the positive x-direction only (the appropriate subscript on θ is also implied). This can be verified by substituting the solution for a wave travelling in the positive x-direction,

$$\phi = A\exp(i(\omega t - kx - \ell y)),$$

where (e.g. Higdon, 1990)

$$\frac{ck}{\omega} = \cos\theta,$$

into (15).

Using (15), estimates are obtained for θ_p and θ_s. These estimated values can then be used in (11) and (13), and this completes the boundary condition.

Anticipated advantages of the ABC

The theory developed in this article does not involve any approximations: (11) and (13) are exact for simple plane waves. The ABC is also local, as the boundary traction at any one node and time step depends only on the solution at the same node and time step, and a few neighbouring points in time and space.

In current practice, the seismic motion is usually specified at the base of the model as vertically propagating S- and P-waves. The boundary condition at the lateral edges of the model is often the viscous boundary due to Lysmer and Kuhlemeyer (1969). Unless the free-field motion is somehow accounted for (which is not straightforward; see Nielsen (2006) or Kontoe et al. (2008) for possible solutions), the viscous boundary will attenuate the seismic motion as it travel up thought the model. This phenomenon is due to leakage of energy through the viscous boundary. The ABC proposed in the present article allows the free-field motion to travel undisturbed towards the surface: for $\theta = 90°$ in (11) and (13), the boundary tractions are the same as those applied by a free-field column (Nielsen, 2006). Therefore, leakage should not occur.

The ABC presented in this article is best paired with an explicit integration code, although it might be possible to use implicit integration as well (see below for an important caveat). The ABC is well suited for FE implementation. Some effort is required to evaluate Δ and ϖ and their derivatives, if (15) is used, at the boundary. However, the highest derivative of the primary solution variables is second-order, and this should not pose any serious challenges. The ABC achieves the complete separation of S- and P-wave components. Until now, this was only possible through potential formulations (e.g. Randall, 1988) which are not easily adapted to FE codes.

3D applications are possible, although the derivation and implementation would likely require some effort.

Anticipated problems

It is uncertain at this stage how the ABC performs when complex waveforms are present. If, for instance, two plane waves approach the boundary with different angles of incidence, does the method break down or would (15) estimate an appropriate 'effective' angle of incidence, leading to cancellation of all reflections? Another option is suggested by the fact that any waveform can be written as a superposition of plane waves. Then the task is to find the plane wave components of the incident wave field, estimate the angle for each component, and then apply the total surface traction as a sum of corresponding 'plane' tractions. However, this may seriously impair the speed and overall attractiveness of the method.

It is a requirement that $-1 \leq \cos\theta \leq 1$. However, due to the approximate nature of numerical analysis, the evaluation of $\cos\theta$ may not fall within these limits. What should the FE code do in this case?

If an implicit integration scheme is chosen, it is necessary to evaluate the Jacobian $\boldsymbol{J}$, which is a matrix given by

$$\boldsymbol{J} = -\frac{\mathrm{d}\boldsymbol{R}}{\mathrm{d}\boldsymbol{U}}$$

where $\boldsymbol{R}$ is a vector of nodal forces and $\boldsymbol{U}$ is a vector of nodal displacements. This may not be straightforward considering the rather complex formula for $\cos\theta$ that ensue from (15). In an explicit integration scheme, this problem is avoided.

Finally, the performance of the ABC in an evanescent wave field has yet to be determined.

Conclusion

This article presents the theory for a new absorbing boundary condition. However, no numerical results have been obtained to validate the theory. The author wishes to contact people who would be interested in undertaking the programming of the required FE code, validation (or refutation?) of the theory, and other related studies. It is believed that this work could be suitable material for final year MSc project (which the author would be willing to co-supervise) or form part of a related PhD project.

References

Cohen, M. and Jennings, P. (1983), Silent boundary methods for transient analysis, *in* T. Belytschko and T.J.R. Hughes, ed., 'Computational Methods for Transient Analysis', Elsevier Science.

Guddati, M. (2006), 'Arbitrarily wide-angle wave equations for complex media', *Computer Methods in Applied Mechanics and Engineering* **195**, 65 – 93.

Higdon, R. (1990), 'Radiation boundary conditions for elastic wave propagation', *SIAM Journal on Numerical Analysis* **27**(4), 831 – 870.

Kellezi, L. (2000), 'Local transmitting boundaries for transient elastic analysis', *Soil Dynamics and Earthquake Engineering* **19**, 533 – 547.

Kontoe, S., Zdravkovic, L. and Potts, D. (2008), 'An assessment of the domain reduction method as an advanced boundary condition and some pitfalls in the use of conventional absorbing boundaries', *International Journal for Numerical and Analytical Methods in Geomechanics* . Published online.

Lindman, E. (1975), 'Free space boundaries for the scalar wave equation', *Journal of Computational Physics* **18**, 66 – 78.

Love, A. (1944), *A Treatise on the Mathematical Theory of Elasticity*, 4th edn, Dover Publications.

Lysmer, J. and Kuhlemeyer, R. (1969), 'Finite dynamic model for infinite media', *Proc. ASCE, Journal of the Engineering Mechnanics Division* **95**(EM4), 859 – 876.

Mulder, W. (1997), 'Experiments with higdons absorbing boundary conditions for a number of wave equations', *Computational Geosciences* **1**, 85 – 108.

Nielsen, A. (2006), Absorbing boundary conditions for seismic analysis in ABAQUS, *in* 'Proceedings of ABAQUS Users' Conference', Boston, MA.

Randall, C. (1988), 'Absorbing boundary conditions for the elastic wave equation', *Geophysics* **53**(5), 611 – 624.

Wolf, J. (1988), *Soil-structure Interaction Analysis in Time Domain*, Prentice Hall.

Wolf, J. (1994), *Foundation Vibration Analysis Using Simple Physical Models*, Prentice Hall.

Forthcoming events

Date	Venue	Title	Organiser
17/11/2008 at 18:00	Institution of Civil Engineers One Great George Street, Westminster, London	Dams and Earthquakes	ICE British Dam Society
26/11/2008 at 18:00	Institution of Civil Engineers One Great George Street, Westminster, London	Vibration Servicability of Floors	Ahmed Elghazouli (Imperial College London)
05/12/2008 at 9:00	Institution of Civil Engineers One Great George Street, Westminster, London	One day seminar: Seismic Analysis Using Finite Elements (see also page 7)	Paul Greening (University College London)
10/12/2008 evening	Institution of Structural Engineers 11 Upper Belgrave Street London	GEM: the Global Earthquake Model - A Public-Private Partnership. Speaker: Ross S. Stein (U.S. Geological Survey)	SECED/IStructE joint evening meeting
28/01/2009 at 18:00	Institution of Civil Engineers One Great George Street, Westminster, London	Hybrid Testing in Earthquake Engineering	Paul Greening (University College London)
25/02/2009 at 18.00	Institution of Civil Engineers One Great George Street, Westminster, London	High mass, low velocity impact. Speaker: Ian May (Heriot-Watt University)	Andrew Mair (Jacobs)

For further information please contact Pauline Arundel, Engineering Department, at the ICE, on tel. 020 7665 2236 or email Pauline.arundel@ice.org.uk. Visit the SECED website at http://www.seced.org.uk.

Seismic Analysis using Finite Elements

A one-day seminar in London, 5 December 2008

Modern numerical analysis methods provide a valuable tool to engineers involved in the design or assessment of mechanical, structural and geotechnical systems which may experience earthquake loads. Finite element analysis methods are firmly established as the most powerful method for simulation of structural response to seismic actions. Safe and effective use of FE methods for seismic analysis requires a good understanding of structural mechanics, as well as knowledge of the capabilities and limitations of special purpose analysis methods. An appreciation of engineering seismology is also valuable.

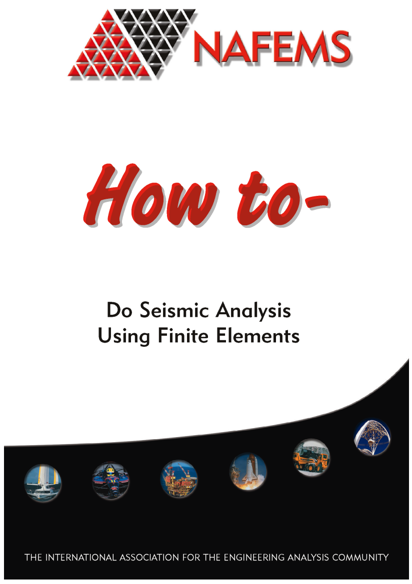

This one day seminar brings together experienced specialists from industry and academia to present examples of recent use of FE methods for seismic analysis. The objective of the event is to provide practical insight into the application of a variety of FEA tools to a range of earthquake engineering challenges. The emphasis will be on effective use of readily available analysis methods, rather than cutting-edge research activity.

This seminar is jointly organised with NAFEMS, an independent, international authority on the use of computer modelling and simulation methods. NAFEMS is a vendor neutral, not-for-profit membership association of more than 800 companies from all over the world. Members range from major corporations such as Boeing through mid-sized organizations such as JCB, to small-scale engineering consultants.

The seminar accompanies the introductory book "How to do Seismic Analysis using Finite Elements", recently published by NAFEMS.

Upon registration, attendees will have the opportunity to purchase this publication for the heavily discounted price of £5. Details will be provided with your registration confirmation.

To register, visit http://www.nafems.org/seismic. For information about the technical contents, contact Paul Greening (Paul.Greening@ucl.ac.uk).

Venue
The Institution of Civil Engineers
One Great George Street
Westminster, London, SW1P 3AA

Preliminary programme

Title of presentation	Speaker	Affiliation
Welcome		
The nature of earthquakes and their effects on structures	Professor Julian Bommer	Imperial College
Defining earthquake loading	Ian Smith	Atkins
Coffee		
Modelling dynamic soil-structure interaction	Dr Rob May	Atkins
Boundary conditions for seismic analysis	Andreas Nielsen	Jacobs
Lunch		
Tall buildings	Rob Smith	Arup
Stack stability	Rory Lennon	Royal Haskoning
Coffee		
Geotechnical structures	Dr Rob May (TBC)	Atkins
Bridges – The Dubai Metro	Phil Cooper	Intec

A Summary of Earthquakes in 2007

Davie Galloway
British Geological Survey, Edinburgh

This year was quite exceptional in terms of the number of large worldwide earthquakes (Figure 1), relative to the number of deaths which they caused. There were four 'great' earthquakes (magnitude over 8.0), fourteen 'major' earthquakes (magnitudes between 7.0 and 7.9) and 175 'strong' earthquakes (magnitudes between 6.0 and 6.9). These numbers are higher than the long-term averages for these magnitude ranges, which are, one, seventeen and 134, respectively. The number of people reported killed by earthquakes during 2007 was 721 (Table 1), which is significantly less than in the previous three years; 6,569 killed in 2006, 76,649 in 2005 and over 284,000 in 2004.

Most Significant

The majority of the fatalities in 2007 (nearly 72%), occurred as a result of a magnitude M_W 8.0 earthquake on 15 August, approximately 40 km offshore Chincha Alta in the Department of Ica, Peru. Some 519 people were killed, over 1,000 others were injured and around 95,000 buildings and houses were either destroyed or damaged. The majority of the damage and casualties were concentrated in the cities of Ica, Chincha Alta and Pisco. Most of the buildings destroyed were adobe housing and the buildings that sustained the most damage were hospitals, schools, clinics and many other large public buildings. The Pan American Highway and other main transport links also suffered heavy damage mainly due to landslides. The earthquake occurred at the boundary between the Nazca and South American tectonic plates, which are converging towards each other at a rate of about 8 cm per year. It occurred as thrust faulting on the interface between the two plates, with the South American plate moving up and seaward over the Nazca plate. Coastal Peru has a his-

Date	LAT	LON	MAG	Location	Deaths
21 January	1.07 N	126.28 E	7.5	Molucca Sea	4
6 March	0.49 S	100.50 E	6.4	Southern Sumatra, Indonesia	70
25 March	37.34 N	136.59 E	6.7	Honshu, Japan	1
1 April	8.46 S	157.04 E	8.1	Solomon Islands	52
21 April	45.24 S	72.65 W	6.2	Aisen, Chile	10
2 June	23.03 N	101.05 E	6.1	Yunnan, China	3
16 July	37.54 N	138.45 E	6.6	Honshu, Japan	9
21 July	38.94 N	70.49 E	5.2	Tajikistan	15
2 August	47.12 N	141.80 E	6.2	Tatar Strait, Russia	2
15 August	13.39 S	76.60 W	8.0	Central Peru coast	519
12 September	4.44 S	101.37 E	8.4	Southern Sumatra, Indonesia	25
26 October	35.30 N	76.75 E	5.3	Northwest Kashmir	1
6 November	21.18 N	70.72 E	5.0	Gujurat, India	1
7 November	9.72 N	124.65 E	5.1	Bohol, Philippines	1
14 November	22.25 S	69.89 W	7.7	Antofagasta, Chile	2
25 November	8.28 S	118.34 E	6.5	Sumbawa, Indonesia	3
29 November	14.97 N	61.26 W	7.4	Martinique	1
9 December	15.05 S	44.23 W	4.9	Minas Gerais, Brazil	1
20 December	39.01 S	178.29 E	6.6	North Island, New Zealand	1
					721

Table 1. Earthquakes causing deaths in 2007

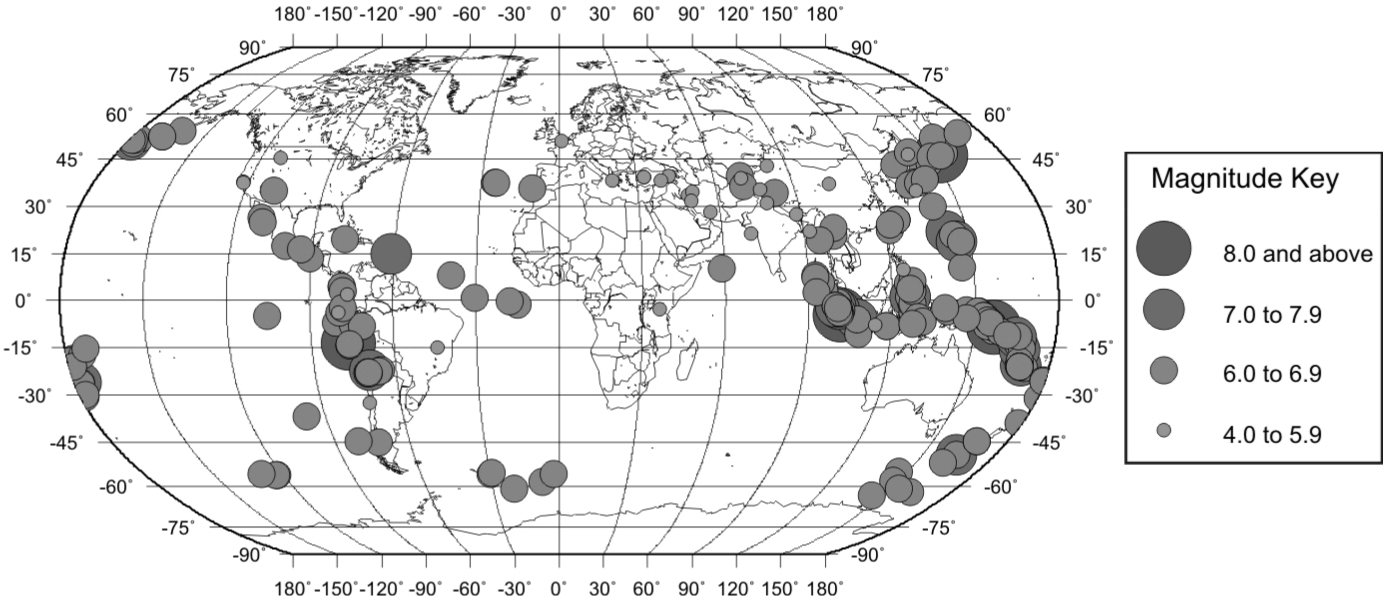

Figure 1. Worldwide seismicity (magnitude 6 and above) and other significant earthquakes in 2007

tory of very large earthquakes. The 15 August event locates in the same general region as a magnitude M_W 8.1 earthquake on October 1974 and a magnitude M_W 7.7 in August 1942. It is also located approximately 700 km northwest of the magnitude M_W 9.0 earthquake, the largest coastal Peru earthquake of the last two centuries, which occurred on 13 August 1868 and which produced a tsunami that killed thousands of people along the South American coast and also caused damage in Hawaii.

The largest earthquake during the year, with a magnitude of M_W 8.4, occurred on 12 September and was the first in a series of earthquakes to strike the coastal region of southern Sumatra, Indonesia. Another two "major" earthquakes (magnitudes between 7.0 and 7.9) struck the region soon after. The first occurred later the same day with a magnitude of M_W 7.9 and the second occurred the following day, 13 September, with a magnitude of M_W 7.0. At least 25 people were killed, 161 others were injured and over 56,000 homes were destroyed or damaged in Bengkulu and West Sumatra, as a result of these earthquakes. They were felt strongly throughout the region as far away as Singapore, nearly 700 km from the epicentre. The magnitude M_W 8.4 event locates approximately 1,000 km southeast of the magnitude M_W 9.3 Sumatra earthquake of 26 December 2004, which killed over 284,000 people. They occurred as the result of thrust faulting on the boundary between the Australia and Sunda plates. At the location of these earthquakes, the Australia plate moves northeast with respect to the Sunda plate at a rate of about 6 cm per year.

Two other fatal and damaging earthquakes occurred in the same general region of southern Sumatra, Indonesia during 2007. They both occurred on 6 March, within two hours of each other, with magnitudes of M_W 6.4 and 6.3. They caused the deaths of at least 70 people, injured 826 more and destroyed or damaged over 43,700 homes in the cities of Bukittinggi, Payakumbuh, Solok and Padang in the Province of West Sumatra. The locations and focal-mechanisms of the earthquakes are consistent with these shocks occurring on the Sumatran fault, a 1,900 km long strike-slip fault that extends the length of the island.

Others

A damaging M_W 7.5 earthquake, in the Molucca Sea region, on 21 January, resulted in the deaths of four people, injured scores more and caused minor damage to several buildings. All the damage and casualties occurred on Manado, the capital of the North Sulawesi province of Indonesia, approximately 150 km west of the epicentre.

Near the west coast of Honshu, Japan, on 25 March, an earthquake with a magnitude of M_W 6.7, killed one person, injured 279 more and damaged or destroyed over 6,000 buildings on the Noto Peninsula. Water, power and transport systems were severely disrupted in the region and over 60 landslides were reported. A tsunami warning was issued immediately for the Noto Peninsula and nearby coastal areas, and waves of 10-20 cm were observed 30-45 minutes later. Agriculture, forestry and fishery losses were estimated at approximately US$50 million as a result of this earthquake and associated tsunami.

On 1 April, an earthquake with a magnitude of M_W 8.1 occurred in the Solomon Islands triggering a destructive tsunami. The earthquake and associated tsunami caused the deaths of at least 52 people (with many others still reported missing), injured hundreds more and destroyed several villages in the area. Most of the casualties were reported to be from Gizo, where 500 homes were damaged and Sasamunga, where over 300 homes were damaged and a hospital was destroyed. Tsunami damage also occurred on Woodlark Island, Papua New Guinea where 17 houses were destroyed and a church was damaged. The earthquake was caused by the underthrusting of the Australia/Woodlark/Solomon Sea plate beneath the Pacific plate, as part of the wider northeast directed subduction process. The Solomon Islands arc as a whole experiences a very high level of earthquake activity, and many earthquakes of magnitude 7.0 and above have been recorded in previous years.

A magnitude M_W 6.2 earthquake occurred on 21 April in the Aisen region of Chile, resulting in the deaths of 10 people, who were all swept away by massive 7 metre waves caused by rockslides falling into a narrow fjord near Puerto Aisen.

On 2 June, a magnitude M_W 6.1 earthquake occurred in the Yunnan Province of China, near the borders of Myanmar, Laos and Vietnam. Three people were killed and about 400 more were injured. Many houses collapsed and a number of reservoirs, power plants, bridges and railways were also damaged in the Ning'er area. Several roads were also blocked in the region as a result of either mudslides or rockslides. Damage has been estimated at around US$350 million.

Two other 'strong' earthquakes occurred in Japan during 2007. The first occurred near the west coast of Honshu, on 16 July with a magnitude of M_W 6.6. Nine people were killed, over 1,000 more were injured, nearly 900 houses were damaged, many roads and bridges were damaged and several landslides were reported in Nagano, Niigata and Toyama Prefectures. The earthquake occurred in a zone of compressional deformation that is associated with the boundary between the Amur and the Okhotsk plate, which are relatively small plates that lie between the Eurasian and the Pacific plate. The second, with a magnitude of M_W 6.8, occurred approximately thirteen hours later with an epicentre in the Sea of Japan.

On 21 July, an earthquake with a magnitude of M_W 5.2, occurred in Tajikistan. It killed fifteen people, injured scores more and destroyed or extensively damaged over 1,500 houses in nineteen villages in the Rasht district, including six schools and several health care facilities. Twelve of the fatalities occurred as a result of a related mudslide in the Asht district of Sughd Province.

An earthquake in the Tatar Strait, Russia, on 2 August, with a magnitude of M_W 6.2, killed two people, injured 12 others and destroyed or damaged 31 buildings in Nevel'sk, Russia. Two days later, on 4 August, another two people were injured as a result of a magnitude M_b 4.9 earthquake in the same locality.

On 26 October, in NW Kashmir, one person was killed and 12 others were injured, as a result of landslides, in Ghanche, Pakistan when a magnitude M_b 5.3 earthquake occurred in the region. The earthquake occurred in the same general region as the magnitude M_W 7.6 earthquake on 8 October, 2005, which killed about 75,000 people, injured more than 76,000 others and left nearly three million homeless.

In Gujurat, India, on 6 November, an earthquake with a magnitude of M_b 5.0, killed one person, injured 5 others and damaged several buildings in the Talala area of Junadagh District.

On 7 November, an earthquake with a magnitude of M_b 5.1, occurred offshore the island of Bohol, Philippines and killed one person in the town of Mabini.

A 'major' earthquake, with a magnitude of M_W 7.7, occurred near Antofagasta, approximately 1,200 km north of the capital Santiago, on 14 November. It killed two people, injured hundreds more and damaged thousands of buildings leaving around 15,000 people homeless. Power and communication outages were reported from throughout the epicentral region. A tsunami was also generated as a result of this earthquake and wave heights of 25 cm and 19 cm were recorded at Antofagasta and Iquique tide stations, respectively. Two 'strong' aftershocks occurred the following day (15 November) at 15:03 and 15:06 UTC with magnitudes of M_W 6.2 and 6.8, respectively. These earthquakes occurred near the southern end of the rupture of the 'great' magnitude 8.8 earthquake in 1877, which caused the deaths of at least 34 people and produced a destructive 24 metre tsunami that caused extensive damage along the Peru-Chile coast and was observed throughout the Pacific Basin including Samoa, New Zealand, Australia, Japan, Mexico and California.

On 25 November, two earthquakes, both with magnitudes of M_W 6.5, occurred within four hours of each other, in the Sumbawa region, Indonesia resulting in the death of three people. Hundreds of others were injured and hundreds of houses were destroyed in the Bima, Dompu and Raba areas.

An earthquake with a magnitude of M_W 7.4, occurred north of the island of Martinique, in the eastern Caribbean Sea, on 29 September. On Martinique, one person was killed, scores more were injured, several buidings collapsed and power outages occurred throughout the island. Another two people were injured and several buildings were destroyed on Barbados and minor damage was reported from St Vincent, St Lucia and Guadeloupe. This is the largest earthquake recorded in the region since a magnitude 7.5 event on 8 October, 1974, which caused considerable damage on Antigua, Barbuda, St Kitts, Montserrat, Nevis and Guadeloupe.

On 9 December, Minas Gerais, Brazil, one person was killed, six others were injured and 76 buildings were damaged leaving 380 people homeless in the towns of Itacarambi and Manga as a result of a magnitude M_b 4.9 earthquake.

A magnitude M_W 6.6 earthquake occurred on 20 December off the east coast of North Island, New Zealand resulting in the death of one person (from a heart attack), causing injury to two others, collapsing three buildings and damaging many others in Gisborne.

UK Earthquakes

There were 111 earthquakes located by the BGS seismic monitoring network during the year, with 38 having magnitudes of M_L 2.0 or greater, twelve having magnitudes of M_L 3.0 or greater and four having magnitudes of M_L 4.0 or greater (Figure 2). Thirteen events with a magnitude of M_L 2.0 or greater were reported felt, together with a further 23 smaller ones, bringing the total to 36 felt earthquakes in 2007.

The largest onshore earthquake of the year with a magnitude of M_L 4.3 occurred in Folkestone, Kent on 28 April at 07:18 UTC, at a depth of about 5 km. BGS received a number of reports via the media, the Police and from a number of residents throughout Kent. Typical reports described "the shaking lasted for approximately 10 seconds, causing all our houses to shake", "the whole experience really scared me", "the whole house was shaking from the roof to the floor" and "a loud noise and then a shaking sensation woke me up". This earthquake was followed by 12 aftershocks with magnitudes between M_L 0.8 and 1.7. A macroseismic survey was launched on the BGS 'Earthquakes' web site, which yielded over 1,000 replies. The most distant felt reports were from Norwich approximately 175 km away and Bognor approximately 130 km away. The earthquake was felt over an area of 8,500 sq km for isoseismals 3-5. In parts of Folkestone, where the highest observed intensity was 6 EMS, many houses suffered minor structural damage to chimneys and walls. Data from a strong motion instrument, not located on bedrock, approximately 5 km from the epicentre suggests that peak ground acceleration (PGA) may have been as large as 0.1 g. While no previous earthquakes have been detected near Folkestone in instrumental times (since 1970), a few historical earthquakes are known to have occurred in the Dover Straits area, namely a M_L 5.8 earthquake in 1382, a M_L 5.8 in 1580 and a M_L 4.1 in 1776. A source mechanism for the Folkestone earthquake was determined. The solution shows a strike slip mechanism with a normal component and either right lateral

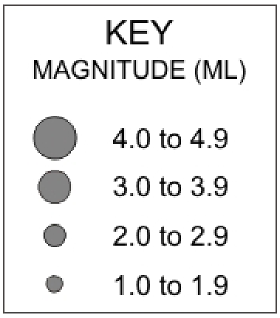

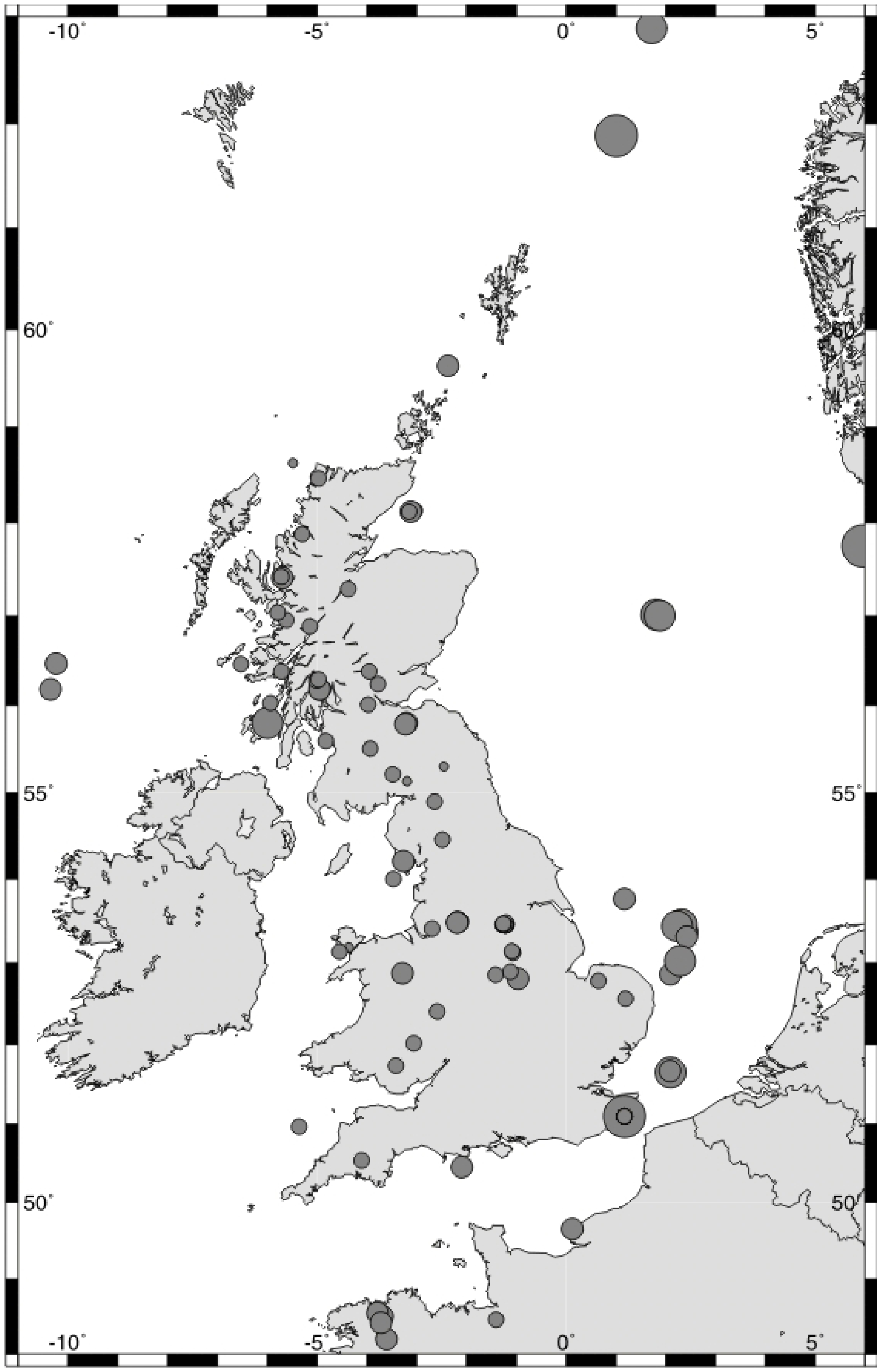

Figure 2. Epicentres of all UK earthquakes located in 2007 (from the Bulletin of British Earthquakes 2007).

movement on a WSW-ENE striking or left lateral movement on a NNW-SSE striking nodal plane. The NNW-SSE striking nodal plane matches the trend of the main faults affecting the Kent Coalfield.

The largest offshore earthquake occurred in the Norwegian Sea on 7 January, with a magnitude of M_L 4.8. It was located approximately 230 km northeast of Lerwick, Shetland Islands. The BGS received several reports from residents in the Shetland Islands which described, “my computer table rocked back and forth” and “the rattle was much more severe and prolonged than I have ever heard before”. On 28 January an earthquake with a magnitude of M_L 4.0 was felt in southern Norway. It occurred in the eastern North Sea region, approximately 50 km southwest of the southern Norwegian Coast. A further 15 events occurred in the North Sea and surrounding waters during the year, with magnitudes ranging between M_L 2.0 and 4.4. Two of these events occurred in the Northern Atlantic Ocean, approximately 170 km northwest of Ireland, on 17 June and 21 July, with magnitudes of M_L 2.2 and 2.7, respectively. These are the first earthquakes in the area since a magnitude M_L 2.9 event on 19 December 1986 and before that a M_L 3.3 event on 13 April 1980.

Two earthquakes, within seconds of each other, were detected on 18 February with epicentres near Lochgoilhead, Strathclyde. They occurred at 20:10:03s and 20:10:14s UTC, with magnitudes of M_L 2.0 and 2.3, respectively. The BGS received a number of reports via the Strathclyde Police and from several residents in the Lochgoilhead area which described “we felt the house shake” and “we felt two distinct rumbles” indicating an intensity of at least 3 EMS. These events are the largest detected in the area since a magnitude M_L 2.9 earthquake near Loch Fyne on 18 May 1996, which was felt with an intensity of 4 EMS.

Between 7 March and 19 April, sixteen events were recorded, with magnitudes ranging between M_L 1.0 and 1.7, in the Maltby area of South Yorkshire. The BGS received reports, for all the events, via Doncaster City Council and from residents in Maltby, typically describing “movement of the house which physically rocked” and “a faint rumbling”. Their shallow depths (around 2 km) and characteristics of their seismograms are similar to previous activity in the area that was associated with mining.

An earthquake with a magnitude of M_L 2.0 and at a depth of 15 km occurred on 8 July, with a location near Millom, Cumbria. The epicentre is approximately 30 km southeast of Sellafield and approximately 90 km south of Chapelcross.

A magnitude M_L 2.6 earthquake occurred on 17 July, with an epicentre about 5 km northwest of Melton Mowbray, Leicestershire. The BGS received a single report from a resident of Kirkby Bellars (3 km south of the epicentre) describing, “a deep roaring noise, immediately followed by the house shaking and the windows rattling”. It locates 8 km WSW of the magnitude M_L 4.1 Melton Mowbray earthquake of 28 October 2001 which was widely felt in the region with a maximum intensity of 5 EMS.

Between 10 and 30 August, six earthquakes were detected in the Manchester area with magnitudes ranging between M_L 1.4 and 2.5. The BGS received reports for all six events via the Media and from residents in the Manchester and Stockport which typically described “the whole house shook and vibrated for a few seconds”, “there was a sudden jolt”, “the building shook violently” and “some people ran into the streets” indicating intensities of between 3 and 4 EMS. They were located in the same region as a series of around 150 events which occurred between October 2002 and January 2003. The largest event in that series, with a magnitude of M_L 3.9, occurred on 21 October 2002 and was felt throughout the region with intensities of at least 5 EMS.

On 17 September, an earthquake with a magnitude of M_L 3.0 was detected 4 km southwest of the settlement of Craighouse, on the southern tip of the Isle of Jura, Argyll. The BGS received information from the local Media, that it was felt on the Isle of Islay and on southern Jura. It locates 28 km south of a magnitude M_L 3.5 earthquake on 3 May 1998, which was felt with intensities of 4 EMS in the area.

Two earthquakes, both with magnitudes of M_L 2.3, occurred in the Penicuik area of Midlothian on 30 November and 9 December. The BGS received several reports from residents in the area that described “the building shook violently”, “we noticed a strong thump from beneath the floor” and “felt a rumbling which lasted no more than a second or two” indicating an intensity of at least 3 EMS. These are the largest earthquakes in the region since a similar magnitude M_L 2.3 event, near Rosewell, on 21 December 1986, which was felt with intensities of 4 EMS.

On 30 November, a magnitude M_L 2.9 earthquake occurred in the Llangollen region of North Wales. The BGS received many reports from as far away as Shrewsbury, 40 km to the southeast and from Ffestiniog, 45 km to the west-northwest, describing “a moderate shaking, enough to make windows rattle” and “we felt and heard a faint rumbling”. An intensity of 4 EMS was assigned to the earthquake. It is located in the same general region (within 20 km) as a magnitude M_L 3.5 earthquake that occurred on 23 January 1974 near Bala, Gwynedd.

Further information

The ‘Bulletin of British Earthquakes 2007’ edited by D D Galloway and previous years’ bulletins can be obtained from BGS Seismology and Geomagnetism or from the Seismology Website at http://www.earthquakes.bgs.ac.uk/. For further details contact: D D Galloway, Seismology and Geomagnetism, British Geological Survey, Murchison House, West Mains Road, Edinburgh, EH9 3LA, Scotland, UK.

Notable Earthquakes January – June 2008

Reported by British Geological Survey

Issued by: Davie Galloway, British Geological Survey, September 2008.
Non British Earthquake Data supplied by: The United States Geological Survey.

Year	Day	Mon	Time UTC	Lat	Lon	Dep km	Magnitude M_L	M_b	M_W	Location
2008	01	JAN	06:32	40.29N	72.99E	6			5.6	KYRGYZSTAN
Hundreds of buildings damaged or destroyed in the Osh area leaving over 5,300 people homeless.										
2008	07	JAN	03:12	0.80S	134.01E	12			5.9	PAPUA, INDONESIA
Six people injured and 22 buildings damaged in Manokwari.										
2008	09	JAN	22:24	35.62N	0.57W	10		4.6		NORTHERN ALGERIA
One person killed and several buildings damaged in Oran.										
2008	09	JAN	22:39	58.20N	1.03E	20	3.1			CENTRAL NORTH SEA
2008	15	JAN	17:52	21.98S	179.54W	484			6.5	FIJI ISLANDS REGION
2008	22	JAN	17:14	1.01N	97.44E	20			6.2	NIAS, INDONESIA
One person killed, five injured and several buildings damaged on Nias.										
2008	27	JAN	13:21	56.97N	5.59W	4	2.3			LOCH MORAR,HIGHLAND
Felt Lochailort (3 EMS).										
2008	03	FEB	07:34	2.30S	28.90E	10			5.9	LAKE KIVU REGION
At least 33 people killed and 517 injured in the Cyangugu region, Rwanda. Another five people killed, 200 injured, around 100 buildings destroyed and over 800 seriously damaged in Bukavu, Democratic Republic of the Congo (DCR).										
2008	05	FEB	23:57	51.77N	0.95W	23	2.0			THAME, OXFORDSHIRE
2008	06	FEB	06:09	23.43N	87.11E	10		4.3		WEST BENGAL, INDIA
One person killed, at least 50 injured and many buildings damaged in the Bankura and Bardhaman Districts of West Bengal.										
2008	08	FEB	09:38	10.67N	41.90W	9			6.9	MID-ATLANTIC RIDGE
2008	13	FEB	20:55	31.73N	51.20E	14		4.9		CENTRAL IRAN
Ten people injured and 70 buildings damaged in Nasirabad, Iran.										
2008	14	FEB	02:07	2.40S	28.92E	10			5.4	LAKE KIVU REGION
One person killed and 65 injured in Kigali, the capital of Rwanda and 44 others injured in Bukavu, DCR.										
2008	14	FEB	10:09	36.50N	21.67E	29			6.9	SOUTHERN GREECE
2008	15	FEB	10:36	33.33N	35.31E	10		5.0		LEBANON
Ten people injured in Beirut, Lebanon.										
2008	20	FEB	08:08	2.77N	95.96E	26			7.4	SIMEULUE, INDONESIA
Three people killed and 27 seriously injured in western Aceh Province, Sumatra.										
2008	21	FEB	02:42	55.14N	7.47W	5	2.4			DONEGAL, IRELAND
Felt County Donegal (3 EMS).										
2008	21	FEB	14:16	41.15N	114.87W	7			6.0	NEVADA
Three people injured, more than 20 buildings heavily damaged and some 700 other buildings slightly damaged in Wells, Elko County, Nevada.										
2008	25	FEB	08:36	2.49S	99.97E	25			7.0	MENTAWAI, INDONESIA
2008	25	FEB	21:02	2.25S	99.81E	25			6.6	MENTAWIA, INDONESIA

Notable Earthquakes (continued)

Year	Day	Mon	Time UTC	Lat	Lon	Dep km	Magnitude M_L	M_b	M_W	Location
2008	27	FEB	00:56	53.40N	0.33W	18	5.2			MARKET RASEN, LINCS
One person injured and many buildings damaged in Lincolnshire and South Yorkshire. Felt widely across England and Wales and as far away as Aberdeen and Ireland, with a maximum intensity of 5-6 EMS recorded at Gainsborough, Lincolnshire. Nine aftershocks were recorded between 27 February and 5 April 2008 with magnitudes ranging between 0.4 and 2.2 ML, none were reported felt. See also SECED Newsletter Vol. 20 No.4 June 2008 and macroseismic intensity map on p. 15.										
2008	03	MAR	09:31	46.41N	153.18E	10			6.5	KURIL ISLANDS
2008	03	MAR	14:11	13.35N	125.63E	24			6.9	PHILIPPINE ISLANDS
2008	20	MAR	22:33	35.49N	81.47E	10			7.2	XINJIANG,CHINA
Over 2,000 homes seriously damaged or destroyed in Yutian, Qira and Lop Counties displacing over 46,500 people.										
2008	23	MAR	08:33	50.38N	6.02W	6	2.4			PENZANCE, CORNWALL
2008	29	MAR	12:51	12.18S	77.16W	51			5.3	CENTRAL PERU
Five homes collapsed in Lima and a rockfall caused injury and vehicle damage along the main coastal highway.										
2008	05	APR	13:57	53.36N	0.33W	22	2.8			MARKET RASEN, LINCS
Felt Market Rasen (3 EMS).										
2008	09	APR	12:46	20.07S	168.89E	33			7.3	LOYALTY ISLANDS
2008	12	APR	00:30	55.66S	158.45E	16			7.1	MACQUARIE ISLAND
2008	16	APR	05:54	51.88N	179.16W	13			6.6	ALEUTIAN ISLANDS
2008	24	APR	12:14	1.18S	23.47W	10			6.5	MID-ATLANTIC RIDGE
2008	01	MAY	00:15	33.86N	48.59E	16		4.5		WESTERN IRAN
Over 100 people injured in Lorestan Province, Iran.										
2008	02	MAY	01:33	51.86N	177.53W	14			6.6	ALEUTIAN ISLANDS
2008	06	MAY	06:25	52.12N	3.89W	5	2.2			LAMPETER, DYFED
2008	07	MAY	16:45	36.16N	141.52E	39			6.8	HONSHU, JAPAN
Several people injured in Chiba, Saitama and Tokyo, Japan.										
2008	09	MAY	21:51	12.52N	143.18E	76			6.7	MARIANA ISLANDS
2008	12	MAY	06:28	31.00N	103.32E	19			7.9	EAST SICHUAN,CHINA
At least 69,226 people killed, another 374,643 injured and 17,923 still missing in Sichuan Province and neighbouring regions. More than 45 million people were affected, 15 million were evacuated and over 5 million were left homeless. The total economic loss has been estimated at around $US 90 billion.										
2008	23	MAY	19:35	7.31N	34.90W	9			6.5	MID-ATLANTIC RIDGE
2008	24	MAY	19:20	4.33N	73.76W	9			5.9	COLOMBIA
Six people killed, by a landslide, in Meta, Colombia.										
2008	25	MAY	08:21	32.57N	105.42E	10			6.0	EAST SICHUAN, CHINA
Eight people killed, 927 injured and at least 4,000 homes destroyed in Sichuan.										
2008	27	MAY	08:37	32.71N	105.54E	10			5.7	EAST SICHUAN, CHINA
Additional damage to around 20,000 houses in Sichuan and Shanxii.										
2008	28	MAY	20:09	54.69N	2.95W	6	2.5			PENRITH, CUMBRIA

Year	Day	Mon	Time UTC	Lat	Lon	Dep km	Magnitude M_L	M_b	M_W	Location
2008	28	MAY	20:09	54.70N	2.96W	7	2.0			PENRITH, CUMBRIA
2008	29	MAY	07:23	59.05N	1.24E	16	2.5			NORTHERN NORTH SEA
2008	29	MAY	15:46	64.00N	21.01W	10			6.3	ICELAND
Around 30 people injured and many buildings damaged in the Selfoss area.										
2008	01	JUN	14:31	59.38S	149.66E	10			6.5	MACQUARIE ISLAND
2008	06	JUN	20:02	35.88N	0.66W	4			5.5	NORTHERN ALGERIA
One person killed, more than 30 injured and several homes either destroyed or damaged in Oran, Algeria.										
2008	08	JUN	12:25	37.96N	21.53E	16			6.3	SOUTHERN GREECE
Two people killed, at least 240 injured and over 1,150 buildings damaged or destroyed in the prefectures of Achaia and Ilia, Greece.										
2008	13	JUN	23:43	39.03N	140.88E	8			6.9	HONSHU, JAPAN
At least thirteen people killed, 357 injured and over 600 buildings damaged in the Furukawa and Morioka areas.										
2008	17	JUN	05:51	32.76N	105.55E	10		4.8		EAST SICHUAN, CHINA
Two people killed and one injured in Shaanxi.										
2008	16	JUN	01:10	51.64N	3.67W	5	1.5			MAESTEG, GLAMORGAN
2008	23	JUN	06:37	58.13N	3.07W	6	2.1			MORAY FIRTH
2008	24	JUN	23:31	58.51N	4.97W	4	1.9			KINLOCHBERVIE
2008	27	JUN	11:40	11.01N	91.82E	17			6.6	ANDAMAN ISLANDS
2008	30	JUN	00:34	56.99N	1.85E	5	2.2			CENTRAL NORTH SEA
2008	30	JUN	06:17	58.22S	22.10W	19			7.0	STH SANDWICH ISLANDS

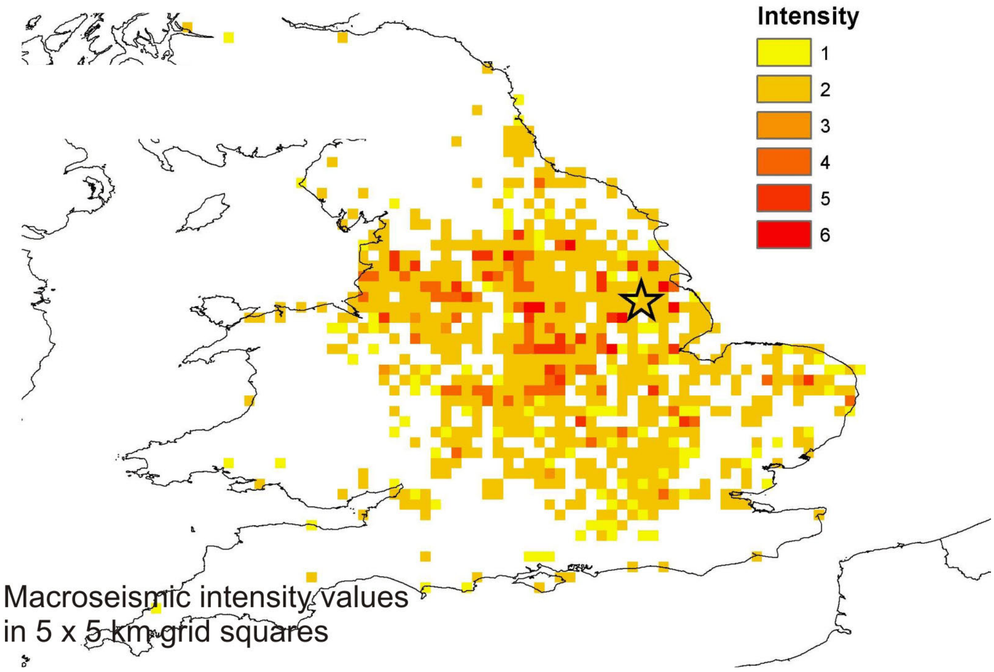

Market Rasen earthquake on 27 February 2008

Winner of the Earthquake Prediction Competition

The winnner of this year's Earthquake Prediction Competition is Andrew Coatsworth who correctly guessed (or otherwise conjectured) that the next major earthquake in the UK would occur in square number 11 (see illustration below), which is where the Penrith earthquake occurred on 28 May at 20:09 with magnitude of 2.5 ML. Mr Coatsworth received a small prize at the recent SECED meeting *Robust Damping in Tall Buildings* (24 September 2008).

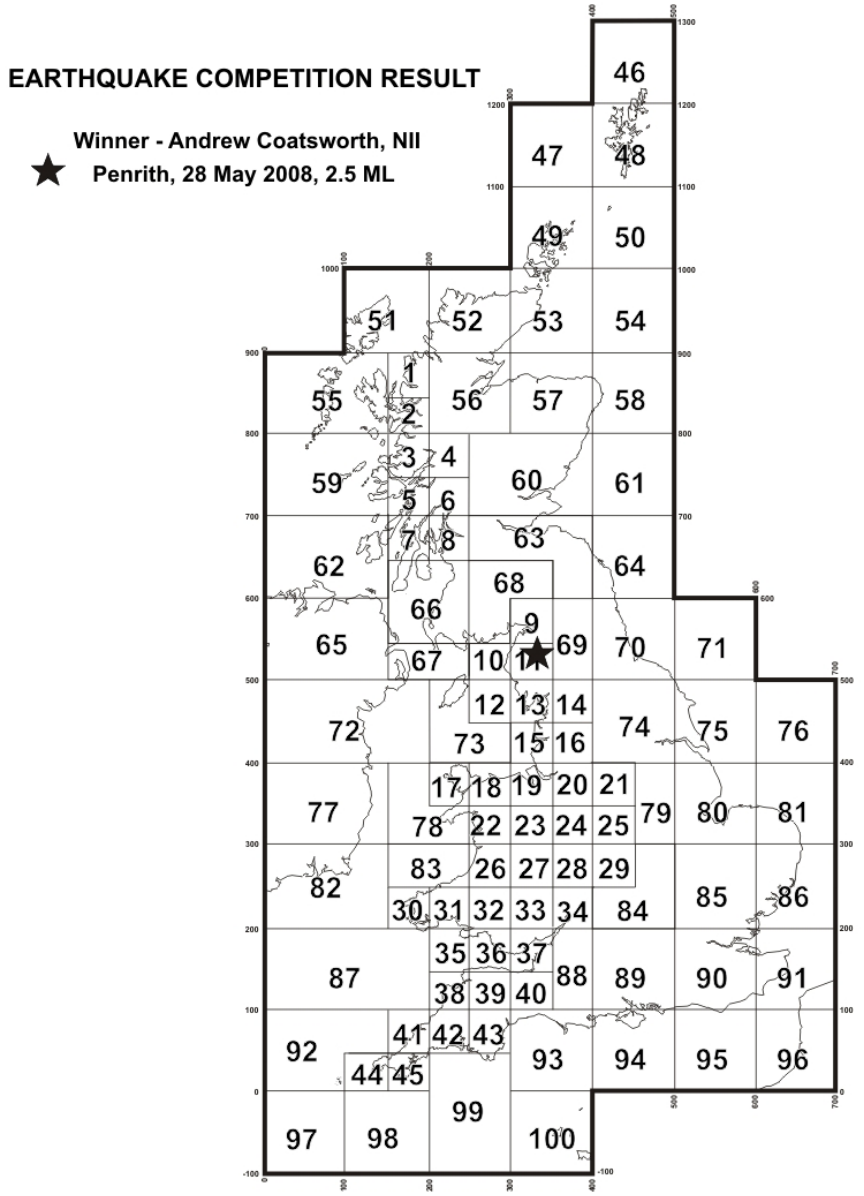

SECED Newsletter

The SECED Newsletter is published quaterly. Contributions are welcome and manuscripts should be sent on a CD or by email. Diagrams, pictures and text should be in separate electronic files. Copy typed on paper is also acceptable. Diagrams should be sharply defined and prepared in a form suitable for direct reproduction. Photographs should be high quality. Colour images are welcome. Diagrams and photographs are only returned to authors on request.

Contributions should be sent to the current editor of the Newsletter, Andreas Nielsen.

Email
andreas.nielsen@jacobs.com

Post
Editor SECED Newsletter
c/o The Secretary
SECED
Institution of Civil Engineers
One Great George Street
London, SW1P 3AA
United Kingdom

SECED

SECED, The Society for Earthquake and Civil Engineering Dynamics, is the UK national section of the International and European Associations for Earthquake Engineering and is an affiliated society of the Institution of Civil Engineers. It is also sponsored by the Institution of Mechanical Engineers, the Institution of Structural Engineers, and the Geological Society. The Society is also closely associated with the UK Earthquake Engineering Field Investigation Team. The objective of the Society is to promote co-operation in the advancement of knowledge in the fields of earthquake engineering and civil engineering dynamics including blast, impact and other vibration problems. For further information about SECED contact:

The Secretary
SECED
Institution of Civil Engineers
One Great George Street
London, SW1P 3AA, UK

Or visit the SECED website:
http://www.seced.org.uk